Electronic Supplementary Material (ESI) for RSC Advances.

Supporting information for:

Effects of Composition and Structure on Performance of Tin/Graphene-Containing Carbon Nanofibers for Li-ion Anodes

Martin K. Dufficy, Sheng-Yang Huang, Saad A. Khan, and Peter S. Fedkiw
Department of Chemical and Biomolecular Engineering, North Carolina State University, Raleigh, NC, USA 27695

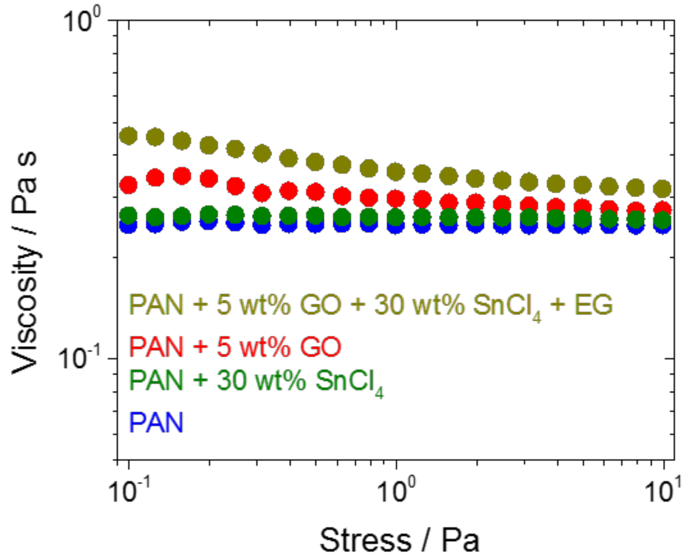

Figure S1. Steady-shear rheology of PAN systems; Experiments were performed to observe the influence of $SnCl_4$ and EG on the viscosity of electrospinning precursor solution. All experiments were conducted with 8 wt% polymer; EG concentration was 4:1 mol EG:$SnCl_4$

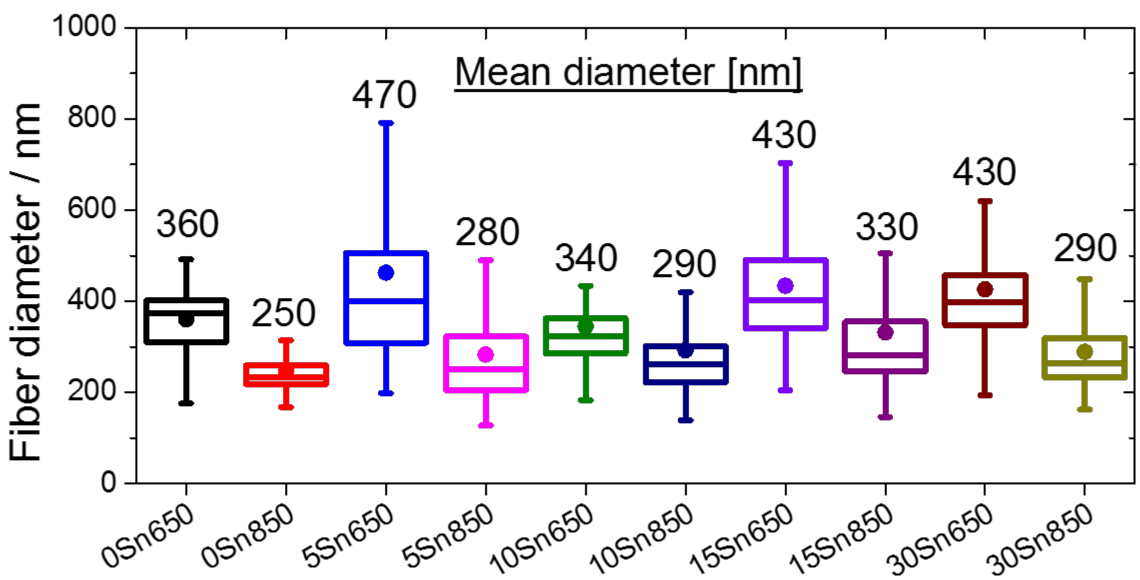

Figure S2. Box plots of fiber diameters for tin-TRGO/CNFs. The dot in each samples represents the mean diameter, which is also written above each individual box plot.

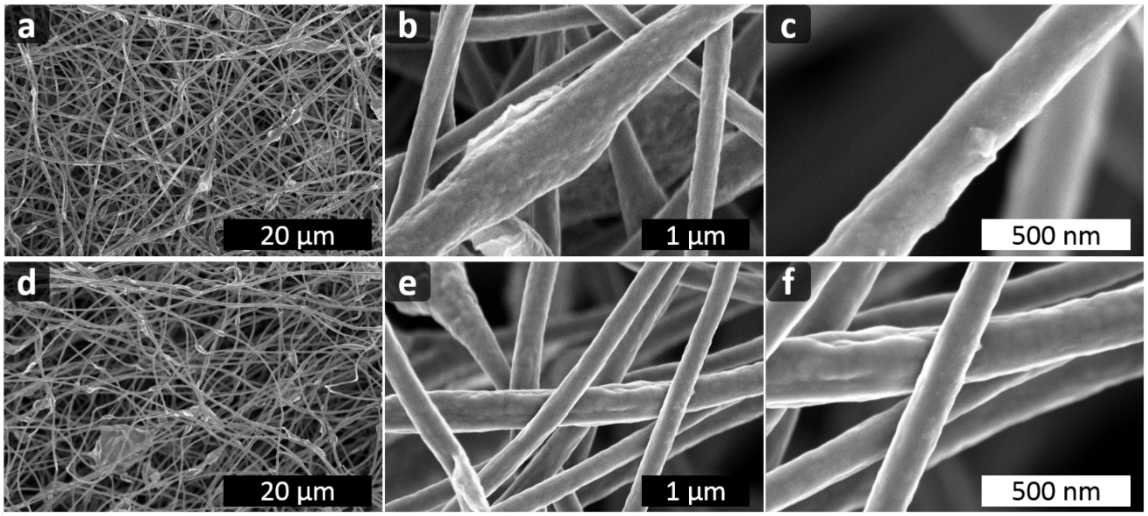

Figure S3. Images of SnO_2-TRGO/CNFs carbonized at 650°C containing a Sn (IV) loadings of (a-c) 5 wt% and (d-f) 10 wt%

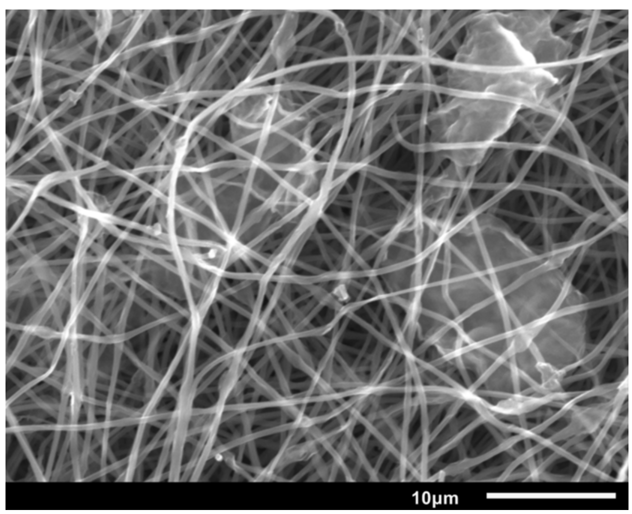

Figure S4. SEM image of TRGO/CNFs carbonized at 850°C

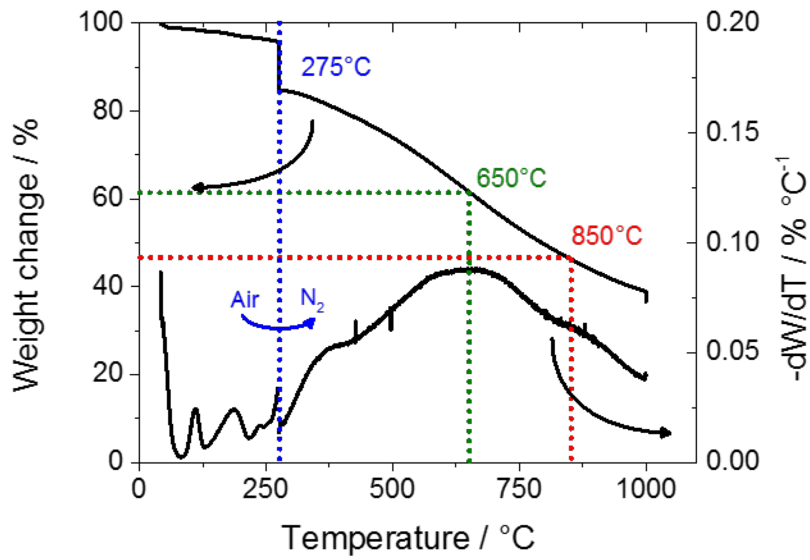

Figure S5. TGA and DTG of GO/PAN fibers. The technique (temperature, heating ramp-rate, and gaseous environment) used for TGA was analogous to stabilization and carbonization of PAN that was used in this study.

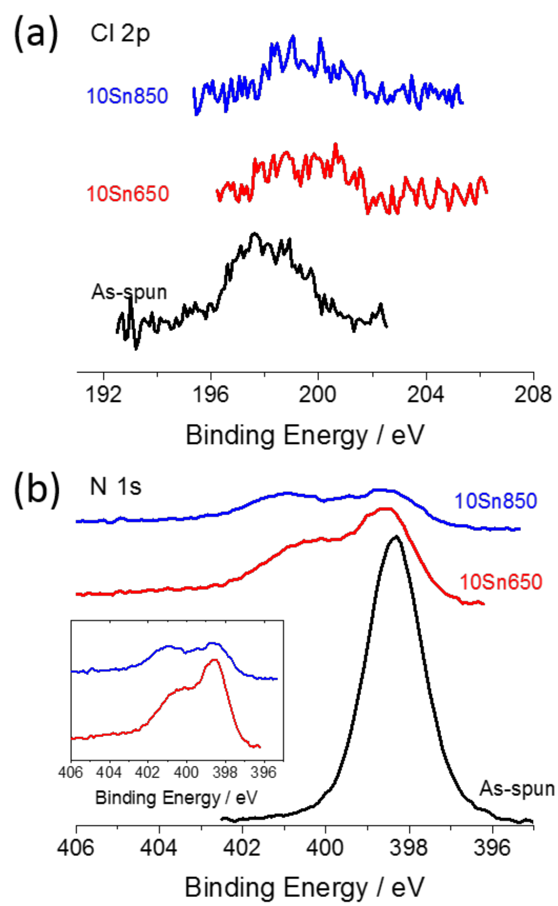

Figure S6. High-resolution XPS transitions of *as-spun* fibers with Sn (IV) loading of 10 wt%, 10Sn650, and 10Sn850 showing (a) Cl 2p and (b) N 1s; the inset of (b) magnifies the N 1s transition of heat treated samples

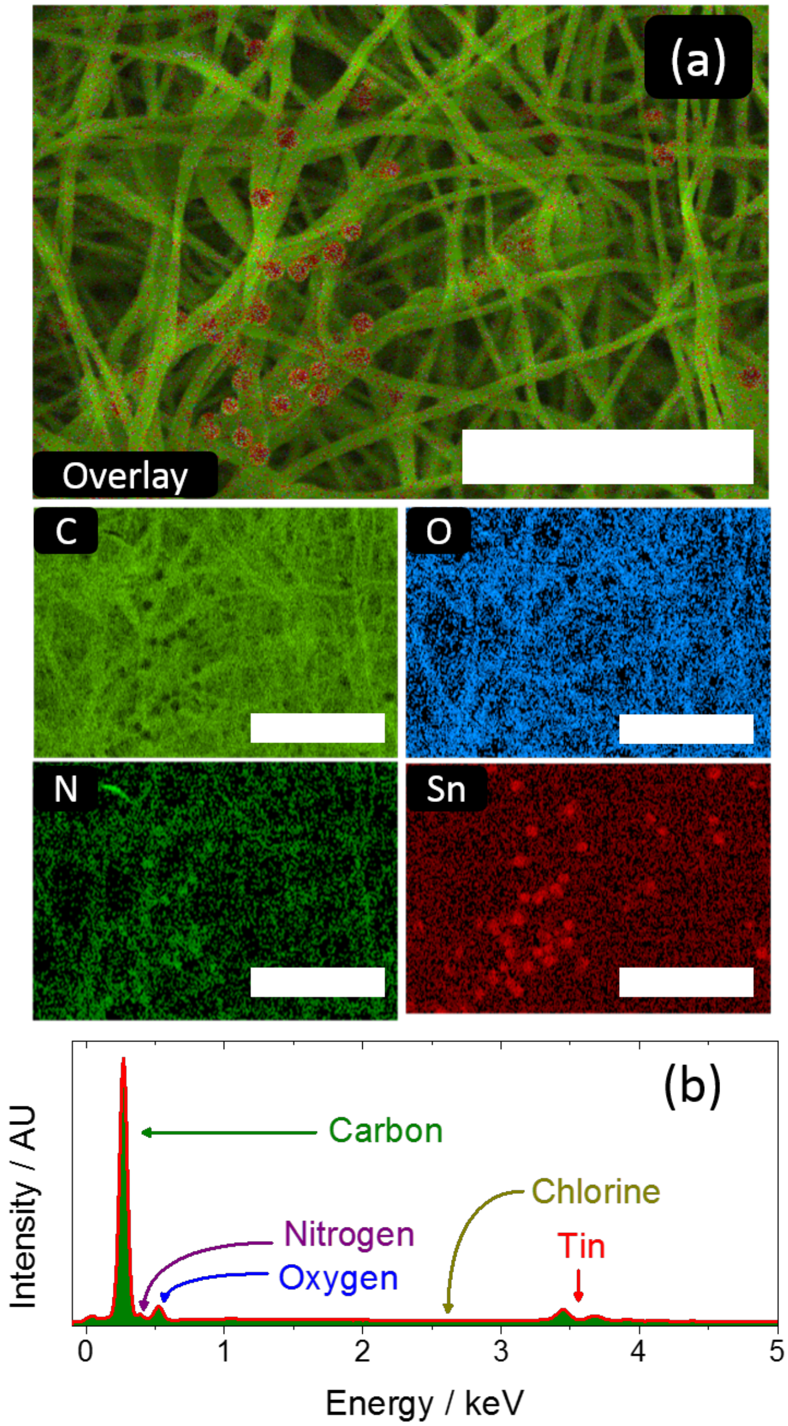

Figure S7. (a) EDS maps overlain on an SEM image of 15Sn850, with individual elemental maps below the overlay. The scale bar represents 10 µm; (b) EDS spectrum of the above sample.

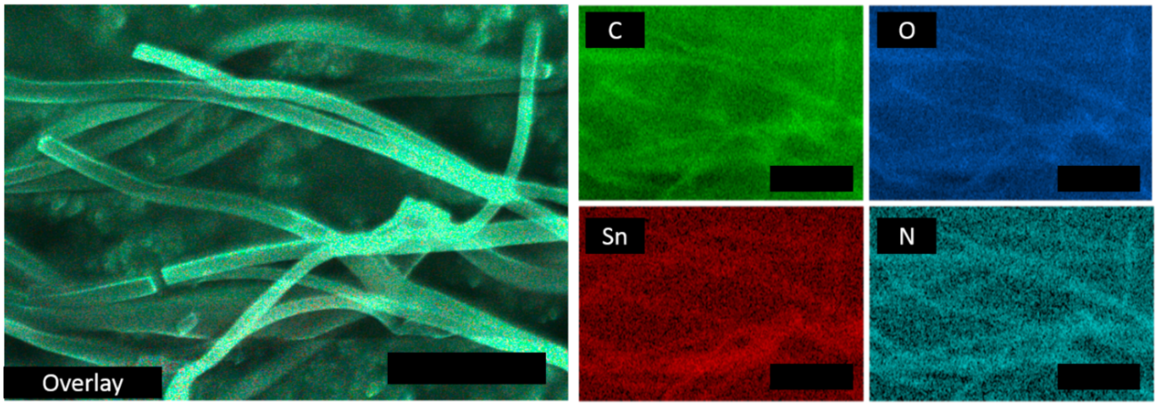

Figure S8. SEM image of 10Sn850 on carbon tape with EDS maps overlain, and the respective elemental maps; Scale bar represents 2.5 μm

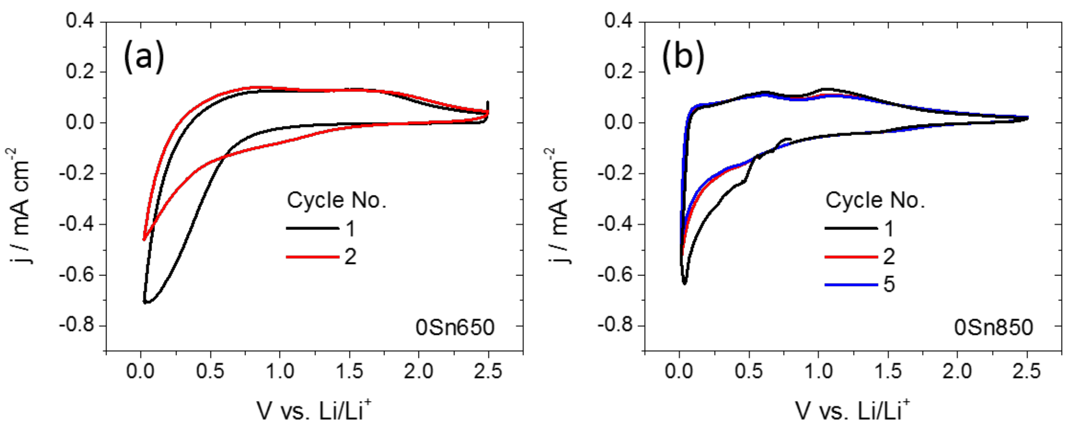

Figure S9. CV of TRGO/CNFs in the absence of tin that were carbonized at (a) 650°C and (b) 850°C

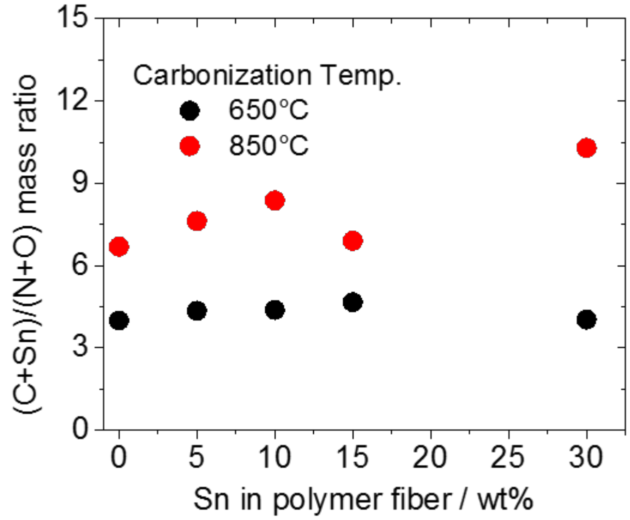

Figure S10. Ratios of Li-reversible to Li-irreversible host materials as measured via EDS.

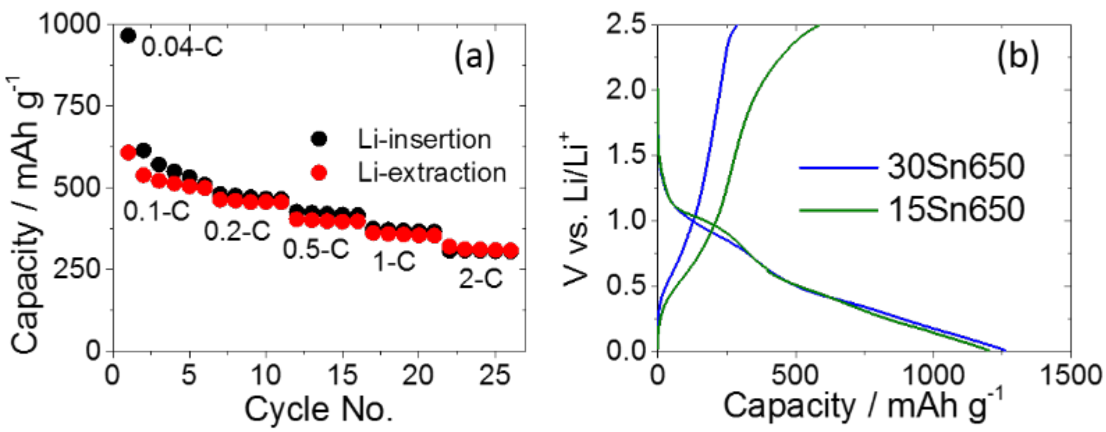

Figure S11. (a) Galvanostatic cycling with potential limitation technique used to calculate *C*-rates as a function of current density; (b) Charge/discharge curves of highly loaded tin electrodes that were carbonized at 650°C

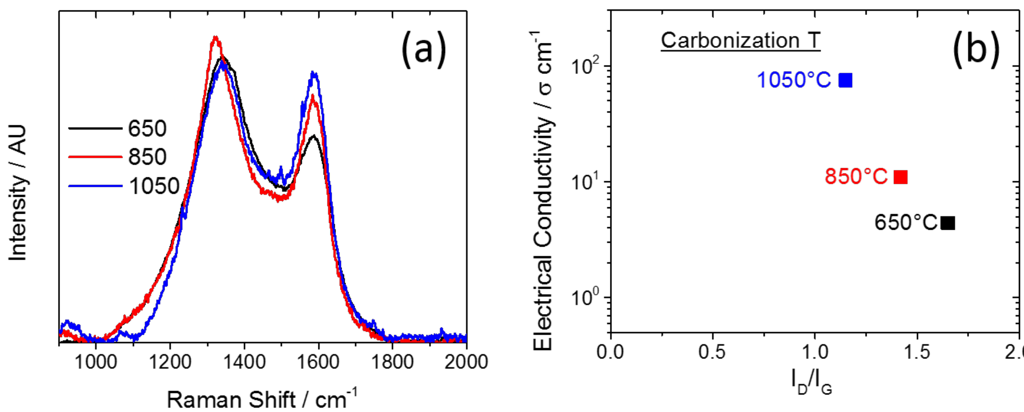

Figure S12. (a) Raman spectra for TRGO/CNFs carbonized at various HTTs; the two peaks in the spectrum above represent the defective (D peak ~1330 cm^{-1}) and graphitic (G peak ~1580 cm^{-1}) nature of TRGO/CNFs. An increased intensity ratio of the two peaks (I_D/I_G) suggests increased disorder in the carbon structure. The I_D/I_G ratios for TRGO/CNFs carbonized at 650, 850, and 1050°C, are 1.65, 1.42, and 1.15, respectively; disorder decreases with HTT. (b) Electrical conductivity of TRGO/CNFs carbonized at different temperatures

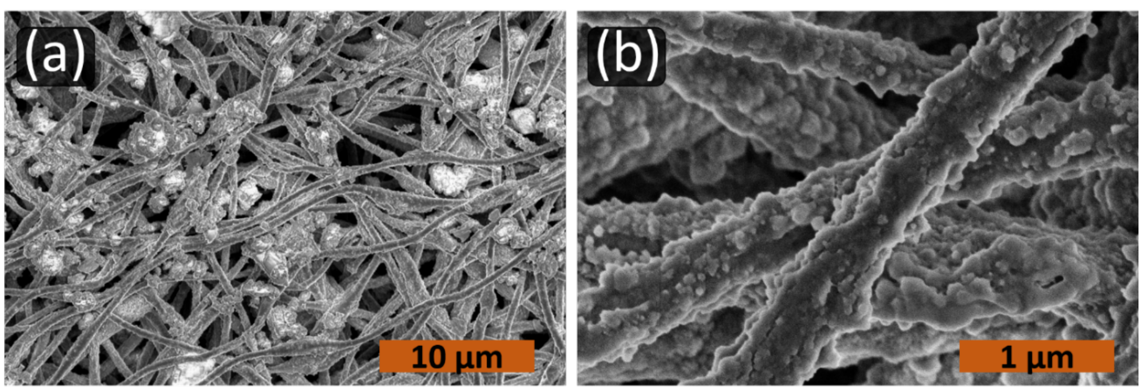

Figure S13. SEM image of 30Sn850 after 500 cycles at 2-*C* at (a) low and (b) high magnification. At low magnifications, we notice that Sn particles aggregate upon cycling, which likely occurred after recurrent pulverizations. After 500 cycles, capacities of TRGO/CNFs with high Sn loadings are equal to capacities in the absence of Sn, which suggests that the Sn deactivates and the fiber structure maintains electrochemical activity.

Tables

Table S1. Coulombic efficiencies, averaged per 100 cycles, corresponding to **Figure 6c**

Cycle Index	CE_{5Sn650} 1-C [%]	$CE_{10Sn650}$ 1-C [%]	CE_{0Sn650} 2-C [%]	CE_{5Sn650} 2-C [%]
100	99.77	100.01	99.9	99.82
200	99.86	99.83	100.03	100.04
300	99.77	99.82	99.98	99.95
400	99.78	99.87	99.95	99.93
500	99.76	99.82	99.93	99.91
600	-	-	99.87	99.90
700	-	-	99.88	99.87
800	-	-	99.89	99.87
900	-	-	99.88	99.88

Table S2. Coulombic efficiencies, averaged per 100 cycles, corresponding to **Figure 6d**

Cycle Index	CE_{0sn850} 2-C [%]	CE_{Sn850} 2-C [%]	$CE_{10Sn850}$ 2-C [%]	$CE_{15Sn850}$ 2-C [%]	$CE_{30Sn850}$ 2-C [%]
100	99.71	99.61	105.9	99.22	99.40
200	99.77	99.66	103.5	99.32	99.70
300	99.75	99.63	101.5	99.34	99.74
400	99.77	99.64	99.94	99.37	99.74
500	99.70	99.65	99.79	99.34	99.75